J|A|C|S
ARTICLES
Published on Web 01/28/2005

N,N′-Linked Oligoureas as Foldamers: Chain Length Requirements for Helix Formation in Protic Solvent Investigated by Circular Dichroism, NMR Spectroscopy, and Molecular Dynamics

Aude Violette,[†] Marie Christine Averlant-Petit,[‡] Vincent Semetey,[†,§] Christine Hemmerlin,[‡] Richard Casimir,[†,||] Roland Graff,[⊥] Michel Marraud,[‡] Jean-Paul Briand,[†] Didier Rognan,[▽] and Gilles Guichard*[,†]

Contribution from UPR 9021 CNRS—Immunologie et Chimie Thérapeutiques (ICT), Institut de Biologie Moléculaire et Cellulaire, 15 rue René Descartes, F-67084 Strasbourg Cedex, Laboratoire de Pharmacochimie de la Communication Cellulaire, UMR CNRS-ULP 7081, 74 route du Rhin, B.P. 24, F-67401 Illkirch, Laboratoire de Chimie-Physique Moléculaire, UMR CNRS-INPL 7568, ENSIC-INPL, BP 451, F-54001 Nancy, and Faculté de Chimie, 1 Rue Blaise Pascal, F-67008 Strasbourg, France

Received September 15, 2004; E-mail: g.guichard@ibmc.u-strasbg.fr

Abstract: *N,N′*-Linked oligoureas with proteinogenic side chains are peptide backbone mimetics belonging to the γ-peptide lineage. In pyridine, heptamer **4** adopts a stable helical fold reminiscent of the 2.6_{14} helical structure proposed for γ-peptide foldamers. In the present study, we have used a combination of CD and NMR spectroscopies to correlate far-UV chiroptical properties and conformational preferences of oligoureas as a function of chain length from tetramer to nonamer. Both the intensity of the CD spectra and NMR chemical shift differences between $^{\alpha}CH_2$ diastereotopic protons experienced a marked increase for oligomers between four and seven residues. No major change in CD spectra occurred between seven and nine residues, thus suggesting that seven residues could be the minimum length required for stabilizing a dominant conformation. Unexpectedly, in-depth NMR conformational investigation of heptamer **4** in CD_3-OH revealed that the 2.5 helix probably coexists with partially (un)folded conformations and that *Z*−*E* urea isomerization occurs, to some degree, along the backbone. Removing unfavorable electrostatic interactions at the amino terminal end of **4** and adding one H-bond acceptor by acylation with alkyl isocyanate (**4** → **7**) was found to reinforce the 2.5 helical population. The stability of the 2.5 helical fold in MeOH is further discussed in light of unrestrained molecular dynamics (MD) simulation. Taken together, these new data provide additional insight into the folding propensity of oligoureas in protic solvent and should be of practical value for the design of helical bioactive oligoureas.

Introduction

Single-stranded and multistranded helices represent a major structural motif in biological macromolecules. Simplified artificial systems based on short-chain synthetic oligomers designed to fold into regular helical conformations[1] provide useful models to study the factors that govern helix formation in these biopolymers. Additionally, helical oligomeric scaffolds may be used for de novo design of molecules with interesting biological activities.[2,3] Intra- and intermolecular self-organization in designed oligomers may result from a variety of noncovalent forces including electrostatic interactions, H-bonds, aromatic−aromatic interactions, coordination to metal ions, steric interactions, or solvophobic effects.[1]

In the realm of peptide mimetics, aliphatic and aromatic ω-peptides as folding oligomers ("foldamers" [4]) have received considerable attention.[1,5] By analogy to natural α-polypeptides, synthetic homooligomers consisting of enantiopure β-amino acids (as short as six residues) adopt, in solution and in the solid state, robust helical conformations maintained by multiple H-bonds and electrostatic interactions.[4,5a−c,e−h] Five helical

[†] Institut de Biologie Moléculaire et Cellulaire.
[‡] ENSIC-INPL.
[§] Current address: Department of Chemistry and Chemical Biology, Harvard University, 12 Oxford St., Cambridge, MA 02138.
[||] Current address: Theraptosis, Pasteur BioTop—Institut Pasteur, 25-28 rue du Dr. Roux, 75724 Paris, France.
[⊥] Faculté de Chimie.
[▽] Laboratoire de Pharmacochimie de la Communication Cellulaire.

(1) For a review, see: Hill, D. J.; Mio, M. J.; Prince, R. B.; Hughes, T. S.; Moore, J. S. *Chem. Rev.* **2001**, *101*, 3893−4011.
(2) Patch, J. A.; Barron, A. E. *Curr. Opin. Chem. Biol.* **2002**, *6*, 872−877.
(3) Selected examples: (a) Patch, J. A.; Barron, A. E. *J. Am. Chem. Soc.* **2003**, *125*, 12092−12093. (b) Arvidsson, P. I.; Ryder, N. S.; Weiss, H. M.; Gross, G.; Kretz, O.; Woessner, R.; Seebach, D. *ChemBioChem* **2003**, *4*, 1345−1347. (c) Wu, C. W.; Seurynck, S. L.; Lee, K. Y.; Barron, A. E. *Chem. Biol.* **2003**, *10*, 1057−1063. (d) Porter, E. A.; Weisblum, B.; Gellman, S. H. *J. Am. Chem. Soc.* **2002**, *124*, 7324−7330. (e) Umezawa, N.; Gelman, M. A.; Haigis, M. C.; Raines, R. T.; Gellman, S. H. *J. Am. Chem. Soc.* **2002**, *124*, 368−369. (f) Rueping, M.; Mahajan, Y.; Sauer, M.; Seebach, D. *ChemBioChem* **2002**, *3*, 257−259.
(4) Gellman, S. H. *Acc. Chem. Res.* **1998**, *31*, 173−180. (b) Appella, D. H.; Christianson, L. A.; Karle, I. L.; Powell, D. R.; Gellman, S. H. *J. Am. Chem. Soc.* **1996**, *118*, 13071−13072.

10.1021/ja044392b CCC: $30.25

shapes (namely, the 3_{14},[4b,6a] 2.5_{12},[6b] $2.7_{10,12}$,[6c] 2.5_{10},[6d] and 2_8 helices[6e]) have been identified in β-peptides depending upon the residue substitution pattern, which illustrates the structural diversity of these synthetic oligomers. Although less studied, their homologues with one additional methylene group inserted into the backbone of each residue, namely, the γ-peptides, have been found to form even more stable helical secondary structures in solution.[5a,b,7] γ^4-, $\gamma^{2,4}$-, and $\gamma^{2,3,4}$-peptide chains as short as four residues adopt a 2.6 helical structure stabilized by H-bonds closing 14-membered pseudocycles. While the α-helix of L-α-peptides and the (*M*)-3_{14} helix of the corresponding β^3-peptides have opposite polarity and helicity,[5a,b,6a] the insertion of two CH_2 groups into the backbone of L-α-amino acids leaves these two helix parameters unchanged, both the α-helix and the 2.6_{14} helix of the resulting γ^4-peptides being right-handed and polarized from the N to C terminus.[7a] In view of these similarities, the γ-peptide helical fold could serve as a template to elaborate functional mimetics of bioactive α-polypeptides.

Prior and parallel to these studies on the conformational preferences of γ-peptides, a number of peptide backbone mimetics belonging to the γ-peptide lineage have been disclosed in the literature including vinylogous peptides (i.e., α,β-unsaturated γ-peptides),[8] oligocarbamates,[9] *N*,*N*′-linked oligoureas,[10,11] oligophosphodiesters,[12] and oligomers of β-aminoxy acids,[13] some of which being able to adopt specific secondary structures. We have shown recently using NMR spectroscopy that the structural information encoded in the γ^4-peptide backbone is partially retained upon substitution of a nitrogen atom for the α-carbon of γ-amino acid residues (Chart 1).[14]

Chart 1

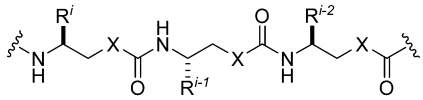

In pyridine-d_5, the resulting enantiopure *N*,*N*′-linked oligoureas adopt a well-defined 2.5 helical structure, reminiscent of the 2.6_{14} helical structure of γ^4-peptides. Like in β- and γ-peptides, the helix of oligoureas is characterized by a stable (+)-synclinal arrangement around the ethane bond. However, the C═O···H−N intramolecular hydrogen bonding pattern is quite different. In oligoureas, the structure is held by H-bonds closing 12- and 14-membered rings formed between C═O(*i*) and N′H($i-2$) and NH($i-3$), respectively. Although our initial studies conducted in pyridine on a heptamer and a nonamer with proteinogenic side chains suggest that oligoureas share a unique three-dimensional fold, the minimal length required for helix formation and the folding propensity of *N*,*N*′-linked oligoureas in protic solvent have not been investigated so far.

Circular dichroism (CD) is a widely applied and convenient spectroscopic technique to investigate the conformation of biopolymers (including proteins and α-polypeptides) and more recently of novel folding oligomers (β-peptides, peptoids, sugar oligomers).[5,15,16] CD should be similarly useful for studying the presence of the $2.5_{12,14}$ helices in oligoureas. Although the nπ* and $\pi\pi$* electronic transitions of the urea chromophore have not been studied as extensively as amides, the contribution of the backbone is expected to dominate the far-UV spectra of enantiopure *N*,*N*′-linked oligoureas in a fashion similar to what is observed for peptides. We found in a preliminary study that the CD spectrum recorded in MeOH (between 195 and 270 nm) of a oligourea nonamer with functionalized side chains displays an intense maximum near 204 nm.[14b] This is in contrast to helical γ^4-peptides that do not exhibit any characteristic CD signature.[7a] However, preferred conformations of novel folding oligomers with chromophores cannot be deduced simply from CD measurements, and complementary NMR studies in the same solvent are usually required to possibly assign a characteristic CD signature to a given conformation.[17] Herein, in an attempt to assess the presence of a regular conformation in protic solvent as well as to correlate far-UV chiroptical properties and conformational preferences of oligoureas, we have undertaken

(5) For reviews, see: (a) Guichard, G. β-Peptides, γ-Peptides and Isosteric Backbones: New Scaffolds with Controlled Shapes for mimicking protein secondary structure elements. In *Pseudopeptides in Drug Development*; Nielsen, P. E., Ed.; Wiley-VCH Verlag: Weinheim, Germany, 2004; pp 33−120. (b) Seebach, D.; Beck, A. K.; Bierbaum, D. J. *Chem. Biodiv.* **2004**, *1*, 1111−1239. (c) Lelais, G.; Seebach, D. *Biopolymers* **2004**, *76*, 206−243. (d) Huc, I. *Eur. J. Org. Chem.* **2004**, 17−29. (e) Seebach, D.; Kimmerlin, T.; Sebesta, R.; Campo, M. A.; Beck, A. K. *Tetrahedron* **2004**, *60*, 7455−7466. (f) Cheng, R. P. *Curr. Opin. Struct. Biol.* **2004**, *14*, 512−520. (g) Cheng, R. P.; Gellman, S. H.; DeGrado, W. F. *Chem. Rev.* **2001**, *101*, 3219−3232. (h) Seebach, D.; Matthews, J. L. *Chem Commun.* **1997**, 2015−2022.

(6) (a) Seebach, D.; Overhand, M.; Kühnle, F. N. M.; Martinoni, B.; Oberer, L.; Hommel, U.; Widmer, H. *Helv. Chim. Acta* **1996**, *79*, 913−941. (b) Appella, D. H.; Christianson, L. A.; Klein, D. A.; Powell, D. R.; Huang, X.; Barchi, J. J., Jr.; Gellman, S. H. *Nature* **1997**, *387*, 381−384. (c) Seebach, D.; Gademann, K.; Schreiber, J. V.; Matthews, J. L.; Hintermann, T.; Jaun, B.; Oberer, L.; Hommel, U.; Widmer, H. *Helv. Chim. Acta* **1997**, *80*, 2033−2038. (d) Claridge, T. D. W.; Goodman, J. M.; Moreno, A.; Angus, D.; Barker, S. F.; Taillefumier, C.; Watterson, M. P.; Fleet, G. W. J. *Tetrahedron Lett.* **2001**, *42*, 4251−4255. (e) Gademann, K.; Häne, A.; Rueping, M.; Jaun, B.; Seebach, D. *Angew. Chem., Int. Ed.* **2003**, *42*, 1534−1537.

(7) (a) Hintermann, T.; Gademann, K.; Jaun, B.; Seebach, D. *Helv. Chim. Acta* **1998**, *81*, 983−1002. (b) Hanessian, S.; Luo, X.; Schaum, R.; Michnick, S. *J. Am. Chem. Soc.* **1998**, *120*, 8569−8570. (c) Hanessian, S.; Luo, X.; Schaum, R. *Tetrahedron Lett.* **1999**, *40*, 4925−4929. (d) Seebach, D.; Brenner, M.; Rueping, M.; Schweizer, B.; Jaun, B. *Chem. Commun.* **2001**, 207−208. (d) Seebach, D.; Brenner, M.; Rueping, M.; Jaun, B. *Chem.—Eur. J.* **2002**, *8*, 573−584.

(8) Hagihara, M.; Anthony, N. J.; Stout, T. J.; Clardy, J.; Schreiber, S. L. *J. Am. Chem. Soc.* **1992**, *114*, 6568−6570.

(9) (a) Cho, C. Y.; Moran, E. J.; Cherry, S. R.; Stephans, J. C.; Fodor, S. P. A.; Adams, C. L.; Sundaram, A.; Jacobs, J. W.; Schultz, P. G. *Science* **1993**, *261*, 1303−1305. (b) Cho, C. Y.; Youngquist, R. S.; Paikoff, S. J.; Beresini, M. H.; Herbert, A. R.; Berleau, L. T.; Liu, C. W.; Wemmer, D. E.; Keough, T.; Schultz, P. G. *J. Am. Chem. Soc.* **1998**, *120*, 7706−7718.

(10) (a) Burgess, K.; Linthicum, D. S.; Shin, H. *Angew. Chem., Int. Ed. Engl.* **1995**, *34*, 907−908. (b) Burgess, K.; Ibarzo, J.; Linthicum, D. S.; Russell, D. H.; Shin, H.; Shitangkoon, A.; Totani, R.; Zhang, A. J. *J. Am. Chem. Soc.* **1997**, *119*, 1556−1564.

(11) Semetey, V.; Didierjean, C.; Briand, J.-P.; Aubry, A.; Guichard, G. *Angew. Chem.* **2002**, *115*, 1975−1978; *Angew. Chem., Int. Ed.* **2002**, *41*, 1895−1898.

(12) Lin, P.; Ganesan, A. *Bioorg. Med. Chem. Lett.* **1998**, *8*, 511−514.

(13) Yang, D.; Zhang, Y.-H.; Zhu, N.-Y. *J. Am. Chem. Soc.* **2002**, *124*, 9966−9967.

(14) (a) Semetey, V.; Rognan, D.; Hemmerlin, C.; Graff, R.; Briand, J.-P.; Marraud, M.; Guichard, G. *Angew. Chem.* **2002**, *115*, 1973−1975; *Angew. Chem., Int. Ed.* **2002**, *41*, 1893−1895. (b) Hemmerlin, C.; Marraud, M.; Rognan, D.; Graff, R.; Semetey, V.; Briand, J. −P.; Guichard, G. *Helv. Chim. Acta* **2002**, *85*, 3692−3711.

(15) (a) Kirshenbaum, K.; Barron, A. E.; Goldsmith, R. A.; Armand, P.; Bradley, E. K.; Truong, K. T. V.; Dill, K. A.; Cohen, F. E.; Zuckermann, R. N. *Proc. Natl. Acad. Sci. U.S.A.* **1998**, *95*, 4305−4308. (b) Wu, C. W.; Sanborn, T. J.; Zuckermann, R. N.; Barron, A. E. *J. Am. Chem. Soc.* **2001**, *123*, 2958−2963.

(16) McReynolds, K. D.; Gervay-Hague, J. *Tetrahedron: Asymmetry* **2000**, *11*, 337−362.

(17) In a case study, Seebach and Van Gunsteren have shown that two β-peptides can differ dramatically in secondary structure and nevertheless display very similar CD spectra. The CD signature typically assigned to the 3_{14} helix might thus not be unique, and unambiguous structural assignment cannot be derived simply from CD measurements. Glattli, A.; Daura, X.; Seebach, D.; van Gunsteren, W. F. *J. Am. Chem. Soc.* **2002**, *124*, 12972−12978.

Chart 2. Oligoureas **1**−**5**

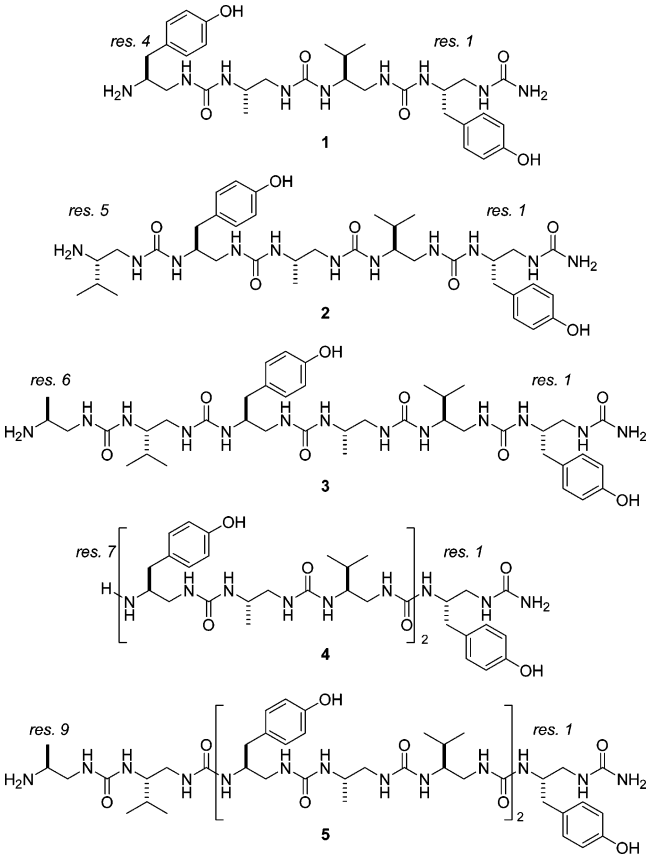

a detailed conformational analysis of enantiopure *N*,*N*′-linked oligoureas of varying length from tetramer to nonamer utilizing both CD and NMR spectroscopy in MeOH as well as CD in trifluoroethanol (TFE).

Results and Discussion

Design and Synthesis of Oligoureas. Heptamer **4** (Chart 2) was previously shown by ^{1}H NMR spectroscopy to adopt a stable $2.5_{12,14}$ helical conformation in pyridine-d_5.[14a] Herein, this sequence with alternating side chains of Ala, Val, and Tyr was used as a basis to design shorter and longer oligomers **1**−**3** and **5**, respectively (Chart 2).

Several approaches have been reported for the preparation of *N*,*N*′-linked oligoureas, all of which involving sequential acylation and amine deprotection cycles using appropriately protected carbonyl synthons.[10,18] Oligoureas **1**−**5** were synthesized on a solid support (Rink amide resin[19]) using *N*-Fmoc-protected succinimidyl carbamates **6** as described previously.[14,18d]

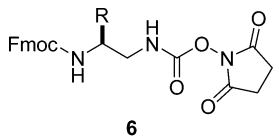

6

R = Me, iBu, 4-tBuOC$_6$H$_4$CH$_2$

The purity of the crude products obtained after cleavage from the resin and lyophilization ranged from 30% (**5**) to 66% (**4**). Oligoureas were purified by C_{18} RP-HPLC and lyophilized. All oligomers were identified by matrix-assisted laser desorption/ionization mass spectrometry (MALDI-MS), and their homogeneity was assessed by C_{18} RP-HPLC (the purity of all peptides determined to be >95%).

By analogy to the α-helix,[20] the orientation of the macrodipole in the 2.5 helical structure suggests that the free NH_3^+ terminus in oligoureas **1**−**5** is helix-destabilizing. In principle, removing the positive charge at the amino terminus by capping could lead to increased helix stability. To overcome the helix-destabilizing effect resulting from repulsive electrostatic interactions between the NH_3^+ terminus in **4** and the positive pole of the 2.5 helix, the free amino group in **4** was acylated by reaction with isopropyl isocyanate (oligomer **7**), and the effect of capping was studied by ^{1}H NMR, CD, and molecular dynamics.

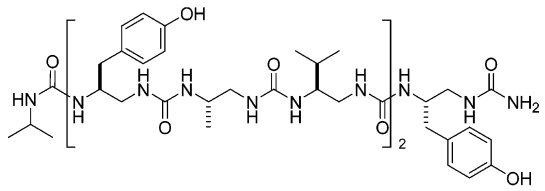

7

Circular Dichroism as a Function of Chain Length. The far-UV (below 250 nm) CD of peptides (α-polypeptides[21] but also new polyamides such as *β*-peptides[5] and peptoids[15]) is dominated by the contribution of the backbone, and different secondary structures will generally give rise to characteristic CD patterns. The main-chain amide, the most abundant chromophore of peptides in the far-UV, is characterized by three electronic transitions: (i) one nπ^* transition at 220 nm polarized along the carbonyl bond, (ii) a $\pi\pi^*$ transition (NV1) at 185−200 nm polarized in the direction of the C−N bond, and (iii) a $\pi\pi^*$ transition (NV2) at 140 nm polarized approximately perpendicular to the C−N bond direction. Interaction between these transitions gives rise to CD spectra of peptides. By analogy, the contribution of the urea chromophore is expected to dominate the far-UV CD spectra of *N*,*N*′-linked oligoureas.

Far-UV CD spectra for tetramer **1**, pentamer **2**, hexamer **3**, heptamer **4**, and nonamer **5** were measured in MeOH between 185/197 and 250 nm at a concentration of 0.5 mM (Figure 1). Tetramer **1** exhibits a CD spectrum with a very weak, broad negative band at ca. 202 nm that qualitatively differs from those of longer oligomers **2**−**5**. CD spectra of oligomers **2**−**5** all display a similar shape with a maximum of positive ellipticity at ca. 203 nm. The intensity of the maximum increases dramatically with the oligomer length from four to seven residues and stabilizes between seven and nine residues to reach a molar ellipticity value per residue of 42000 deg·dmol^{-1} at 203 nm for nonamer **5**, a value close to that previously reported for a nonamer of unrelated sequence.[14b]

To the best of our knowledge, and with the exception of *N*,*N*′-diarylureas,[22] systematic, UV absorption spectra of ureas (i.e.,

(18) (a) Kim, J. M.; Bi, Y.; Paikoff, S.; Schultz, P. G. *Tetrahedron Lett.* **1996**, *37*, 5305−5308. (b) Boeijen, A.; Liskamp, R. M. J. *Eur. J. Org. Chem.* **1999**, 2127−2135. (c) Guichard, G.; Semetey, V.; Didierjean, C.; Aubry, A.; Briand, J.-P.; Rodriguez, M. *J. Org. Chem.* **1999**, *64*, 8702−8705. (d) Guichard, G.; Semetey, V.; Rodriguez, M.; Briand, J.-P. *Tetrahedron Lett.* **2000**, *41*, 1553−1557.

(19) Rink, H. *Tetrahedron Lett.* **1987**, *37*, 3787−3790.

(20) Fairman, R.; Shoemaker, K. R.; York, E. J.; Stewart, J.; Baldwin, R. L. *Proteins: Struct., Funct., Genet.* **1989**, *5*, 1−7.

(21) Sreerama, N.; Woody, R. W. Circular Dichroism of Peptides and proteins. In *Circular Dichroism: Principles and Applications*, 2nd ed.; Berova, N., Nakanishi, K., Woody, R. W., Eds.; John Wiley & Sons: New York, 2000; pp 601−620.

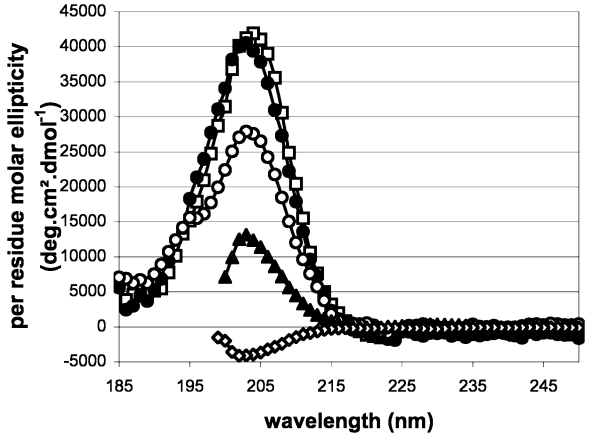

Figure 1. CD spectra of *N*,*N*′-linked oligoureas in MeOH as a function of their chain length: tetramer **1** (◇); pentamer **2** (▲); hexamer **3** (○); heptamer **4** (●); nonamer **5** (□). The spectra were recorded at 293 K.

urea and *N*,*N*′-dialkylureas) have not been investigated in depth, and the electronic transitions of the urea chromophore have not been determined either experimentally or theoretically. One of the reasons is that the absorption bands of urea appear at wavelengths below 190−200 nm. However, thioureas which display transitions at longer wavelength have been well characterized and have been investigated in more detail both experimentally and theoretically.[23] Three bands have been observed in the UV absorption spectra of simple thioureas: a weak band at 280−300 nm and two strong bands at 236−250 and 195−210 nm. These bands have been assigned to an nπ^* transition, a $\pi\pi^*$ transition polarized in the direction of the C_2 axis, and a $\pi\pi^*$ transition polarized perpendicular to this direction, respectively. By analogy, the urea chromophore should then give rise to one nπ^* and two $\pi\pi^*$ transitions, the latter polarized along and perpendicular to the C_2 axis, respectively. Since absorption bands of thioureas have a marked tendency to appear at shorter wavelengths compared to the corresponding bands of thioacetamides,[23a] it is likely that all urea transitions must occur at or below 200−210 nm.[24] Interaction between these transitions in helically disposed urea chromophores could give rise to splittings, and CD bands could appear at higher and lower wavelengths than those corresponding to simple UV transitions, in agreement with the CD spectra presented above for oligomers **2**−**5**. The length-dependent CD signal observed around 203 nm strongly suggests the adoption of one (or more) regular backbone conformation(s) for oligoureas as short as five residues.

In peptides and proteins, however, the four transitions of aromatic side chains of Phe, Tyr, and Trp (namely, L_b, L_a, B_b, and B_a) can make a significant contribution to the far-UV CD spectrum.[25,26] In particular, the positive contribution of aromatic residues (e.g., Tyr) in the 215−230 nm region can lead to an underestimate of the helicity in α-polypeptides.[26] Thus, it could be inferred that phenolic side chains in oligomers **2**−**5** may be responsible for the intense signal observed at 203 nm or for distortion of the CD spectrum. Substitution of alkyl side chains for 4-hydroxybenzyl side chains does not substantially alter the shape and chain length dependence of the CD spectra of oligoureas in the 190−250 nm region (data not shown). This observation suggests that the 203 nm positive band observed in the CD spectra of oligomers **2**−**5** is likely due to the backbone urea chromophore rather than to aromatic transitions; however, the nature of the transition(s) involved still remained to be determined.

To rule out the possibility that intermolecular interactions were responsible for the intense signal at ca. 203 nm, CD spectra were recorded for heptamer **4** at four different concentrations ranging from 5×10^{-4} to 5×10^{-6} M (Figure S10 in the Supporting Information). No significant change either in shape or intensity at 203 nm was observed over this range of concentrations, thus supporting the notion that **4** is largely unassociated in MeOH at 0.5 mM.

^{1}H NMR Study as a Function of Chain Length. To correlate far-UV chiroptical properties and conformational preferences of *N*,*N*′-linked oligoureas as a function of chain length, oligomers **1**−**5** were analyzed by NMR in CD_3OH at a concentration of 3 mM. Spin systems were unambiguously resolved using a combination of DQF-COSY, TOCSY, and HSQC (for heptamer **4** and nonamer **5**) experiments.[27] The sequence-specific assignment of all resonances in the ^{1}H NMR of **2**−**5** (Tables S1−S7 and Figures S2−S6 in the Supporting Information) was achieved by ROESY experiments (mixing time $\tau_m = 350$ ms) and was deduced from the strong N′H($i + 1$)−NH(i) NOE connectivities within each urea bond as exemplified for **5** (Figure 2).[28]

^3J(NH, $^\beta$CH) and ^3J(N′H, $^\alpha$CH) values as well as chemical shift differences ($\Delta\delta$) between diastereotopic $^\alpha$CH protons were found previously to be useful descriptors of the conformational homogeneity of helical *N*,*N*′-linked oligoureas.[14] In pyridine-d_5, helix-forming heptamer **4** exhibits large ^3J(NH, $^\beta$CH) values (≥10 Hz for residues 2−6) that are characteristic of a stable antiperiplanar arrangement between NH and $^\beta$CH. The nonequivalence of diastereotopic $^\alpha$CH protons within central residues results in large $\Delta\delta$ values (in the range 1.3−1.6 ppm) and a strong differentiation between vicinal coupling constants for each pair of diastereotopic $^\alpha$CH protons. This is consistent with their location in a distinct spatial environment and was taken as a hint of a defined secondary structure. Herein, these parameters were extracted for oligoureas **1**−**5** from 1D and 2D ^{1}H spectra recorded at 293 K and compared as a function of chain length (n).

As shown in Figure 3 and with the exception of the amino-terminal residue n, the cluster of $\Delta\delta$ values globally increases

(22) (a) Grammaticakis, P. *Bull. Soc. Chim. Fr.* **1968**, 1057−1070. (b) Boldea, A.; Drugarin, C.; Mracec, M.; Simon, Z. *Rev. Roum. Chim.* **1976**, *21*, 1345−1353.

(23) (a) Hosoya, H.; Tanaka, J.; Nagakura, S. *Bull. Chem. Soc. Jpn.* **1960**, *33*, 850−860. (b) Janssen, M. J. *Recl. Trav. Chim. Pays-Bas* **1960**, *79*, 454−463. (c) Rang, K.; Sandström, J.; Svensson, C. *Can. J. Chem.* **1998**, *76*, 811−820.

(24) Absorption spectra in MeOH of (*S*)-1-isopropyl-3-[2-(3-isopropylureido)-propyl]urea, a model diurea derivative with an aliphatic methyl side chain, and oligomers **1**−**3** all display a large and strong band around 206 nm characteristic of the urea chromophore. Bands at 224 and 278 nm in the spectra of **1**−**3** correspond to the phenolic side-chain transitions L_a and L_b, respectively (Supporting Information).

(25) (a) Manning, M. C.; Woody, R. W. *Biochemistry* **1989**, *28*, 8609−8613. (b) Cooper, T. M.; Woody, R. W. *Biopolymers* **1990**, *30*, 657−676. (c) Woody, R. W. *Eur. Biophys. J.* **1994**, *23*, 253−262. Sreerama, N.; Manning, M. C.; Powers, M. E.; Zhang, J.-X.; Goldenberg, D. P.; Woody, R. W. *Biochemistry* **1999**, *38*, 10814−10822. Woody, A. Y.; Woody, R. W. *Biopolymers* **2003**, *72*, 500−513.

(26) (a) Bhattacharjee, S.; Toth, G.; Lovas, S.; Hirst, J. D. *J. Phys. Chem. B* **2003**, *107*, 8682−8688. (b) Andrew, C. D.; Bhattacharjee, S.; Kokkoni, N.; Hirst, J. D.; Jones, G. R.; Doig, A. J. *J. Am. Chem. Soc.* **2002**, *124*, 12706−12714.

(27) The nomenclature used for the description of backbone and side-chain protons is shown in Figure S1 (Supporting Information).

(28) For short-chain oligomers **1**−**3**, the $\omega\tau_c$ term was not favorable to the establishment of the NOE in NOESY experiments even when the magnetic field $\mathbf{B}_0$ was changed from 300 to 600 MHz.

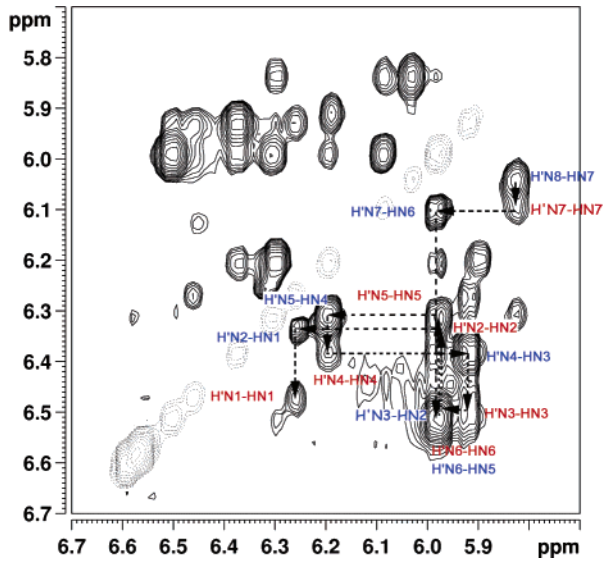

Figure 2. Part of the NH/NH region of the ROESY experiment of **5** recorded at 293 K in CD_3OH. Cross-peaks are in black, and opposite sign diagonal peaks are in gray. NOE cross-peaks between NH(i) and N′H(i) (i = 1−7) are shown in red. Interresidue N′H(i + 1)/NH(i) NOEs (i = 1−7) used for sequence assignment are shown in blue. Residues are numbered consecutively from 1 to 9 as displayed in Chart 2.

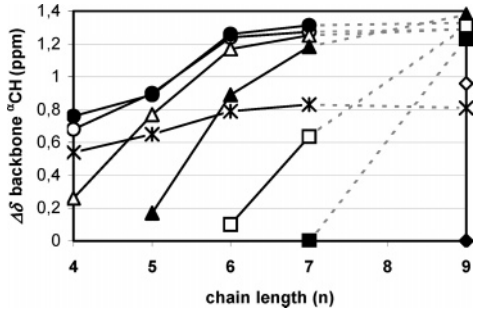

Figure 3. Variation of the chemical shift differences (Δδ) between geminal αCH protons in oligoureas **1**−**5** as a function of chain length (n) as determined from DQF-COSY experiments recorded in CD_3OH at 293 K: residue 1 (∗); residue 2 (○); residue 3 (●); residue 4 (△); residue 5 (▲); residue 6 (□); residue 7 (■), residue 8 (◇), residue 9 (◆).

as a function of chain length. In tetramer **1**, Δδ values for residues 1−3 cluster in the range 0.54−0.76 ppm. Upon addition of one residue (pentamer **2**), the cluster of Δδ values for residues 1−4 increase to 0.65−0.90 ppm. The Δδ value for residue 1 is the least affected by chain length and stabilizes when $n \geq 6$ around 0.8 ppm, a value close to that previously found for this residue in pyridine-d_5 at the same temperature (ca. 0.9 ppm). Also in good agreement with the results obtained in pyridine-d_5 for helical oligoureas,[14] the Δδ values for central residues 2 to $n - 2$ converge to an upper limit of 1.2−1.4 ppm. The amino-terminal residues (n) exhibit low Δδ values ranging from 0.26 in **1** to 0 in **4** and **5**. This behavior is likely to reflect the high mobility of the amino-terminal residue as it is observed in the bundle of the 20 lowest energy conformers of **4** in pyridine-d_5.[14]

Examination of ^3J(NH, $^\beta$CH) values did not revealed any significant chain length dependence, and the observed ^3J values (between 8.5 and 10.9 Hz for oligomers **2**−**5**) suggest that the arrangement between NH and $^\beta$CH is *antiperiplanar* irrespective of n (Table S10 in the Supporting Information). For oligoureas **1**−**4** measurements of ^3J(N′H, $^\alpha$CH) were impossible because

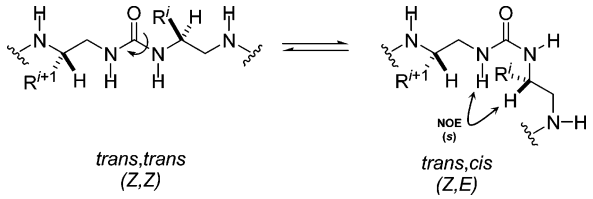

Figure 4. Urea Z−E isomerization leading to strong NOEs between N′H(i + 1) and $^\beta$CH(i) for i = 2−6 observed for **4** in the ROESY experiments recorded in CD_3OH at 286 K.

of the broad lines of their N′H protons in 1D spectra as well as overlaps (Figure S9 in the Supporting Information). Although this latter observation suggested that conformational exchange exists in molecules **1**−**4**, some qualitative evidence for spatial differentiation between the two diastereotopic $^\alpha$CH protons in **4** could nevertheless be inferred from DQF-COSY experiments. For all residues, cross-peaks between N′H and $^\alpha$CH^2 were absent in the DQF-COSY experiment, while a strong cross-peak was always observed between N′H and $^\alpha$CH^1 protons.[29] The thin line width in the spectrum of **5** is certainly in favor of an increased conformational homogeneity. For nonamer **5**, ^3J(N′H, $^\alpha$CH^1) and ^3J(N′H, $^\alpha$CH^2) constants were measured for four residues (measurements for other residues were hampered by severe overlaps). For residues 3, 4, and 7, the presence of large ^3J(N′H, $^\alpha$CH^1) (≥8.9 Hz) and small ^3J(N′H, $^\alpha$CH^2) (≤4 Hz) constants suggests that N′H is nearly antiperiplanar to $^\alpha$CH^1 and synclinal to $^\alpha$CH^2 (Table S11 in the Supporting Information).

Structure Elucidation of 4. Because it was previously found to adopt a regular helical conformation in pyridine-d_5,[14a] heptamer **4** was selected for in-depth conformational analysis in CD_3OH *via* 2-D NMR spectroscopy. In addition, chain-length-dependent CD and NMR studies performed in MeOH (*vide supra*) suggested that seven residues could be sufficient to induce substantial 2.5 helix population in this solvent. Qualitative inspection of the 55 interresidual NOEs collected at 286 K[30] for τ_m = 350 ms (Table S13 in the Supporting Information) revealed the presence of a number of i/i + 2 medium-range NOE connectivities typical for the 2.5 helical structure (i.e., $^\beta$CH(i + 2)/NH(i) and $^\beta$CH(i + 2)/N′H(i) for i = 1, 2, 4, and 5). However, besides this set of NOEs, a number of strong NOE connectivities (e.g., NH(i + 2)/$^\beta$CH(i), N′H(i + 2)/$^\beta$CH(i), N′H(i + 2)/NH(i)) were obviously not compatible with the previously characterized 2.5 helical backbone. In addition, NOEs of strong intensities were observed between N′H(i + 1) and $^\beta$CH(i) all along the backbone (i = 2−6). Interestingly, a short distance between N′H(i + 1) and $^\beta$CH(i) is possible only if one assumes that urea Z−E (*cis*−*trans*) isomerization occurs as shown in Figure 4. For the *Z*,*Z* rotamer and regardless of the geometry of the backbone, the distance between N′H(i + 1) and $^\beta$CH(i) remains larger than 4.0−4.2 Å. Upon urea isomerization the distance between these protons can be shortened to 2.0−2.5 Å. Although *N*,*N*′-disubstituted (thio)ureas generally adopt a *Z*,*Z* conformation, their barriers of rotation as a result of competitive conjugation are lower than

(29) $^\alpha$CH^1 is downfield from $^\alpha$CH^2.
(30) A better dispersion of NH proton resonance was achieved at this temperature compared to 293 K, thus facilitating the interpretation of NOE connectivities.

those of (thio)amides.[31] The formation of stable (thio)urea *Z,E* (*cis,trans*) isomers in apolar solvents has previously been reported in model ureidopeptides[32] as well as in sugar thioureas.[33] Experimentally determined barriers for rotation about the C−N bonds ($\Delta G^{\ddagger}$) for ureas are typically around 11 kcal/mol (13 kcal/mol for thioureas).[31] At the temperatures investigated, NH protons *trans* and *cis* to the oxygen did not give rise to separate signals. The observation of a unique time-averaged peak indicated that rotation about the C−N bonds was particularly rapid, and the *Z,E* to *Z,Z* relative population could not be determined. One can speculate that, in MeOH, each urea bond in **4** can exist as a fast equilibrium between *Z,Z* and *Z,E* conformers, thus leading to a collection of populated conformations folded to various degrees.

As expected, attempts to define the dominant structure(s) of the uncapped heptamer in MeOH from experimentally determined NMR constraints (126 proton−proton distances (intra- and interresidual) and 7 torsion constraints) were unsuccessful as most structures presented large NOE violations and did not converge toward a homogeneous set of conformations. Taken together, this study suggests that, although it is significantly populated, the 2.5 helical structure of **4** in CD_3OH coexists with a certain amount of various partially folded conformations. This might result in part from the additional flexibility of the amino-terminal end of the oligomer in MeOH compared to pyridine which is not able to enforce a stable and consistent helical folding.

Effect of Capping. Removing unfavorable electrostatic interaction at the amino-terminal end of **4** and adding one H-bond acceptor by acylation with isopropyl isocyanate (to give **7**) were believed to enforce a stable and consistent 2.5 helical folding in MeOH that would allow unambiguous NMR structure determination. Conformational differences between capped and uncapped oligomers were first investigated by NMR spectroscopy in CD_3OH at 293 K. Spin system determination and sequence-specific assignment of **7** were performed as described for **4** (see Tables S8 and S9 and Figures S7 and S8 in the Supporting Information). Chemical shift differences $\Delta\delta$ between geminal $^{\alpha}$CH protons in oligourea **7** were determined for residues 1−7 (Figure 5) and compared with the values found in **4**. Although capping did not have a strong influence on $\Delta\delta$ values for residues 1−5, it resulted in an increase of the $\Delta\delta$ values for both ultimate and penultimate residues, thus indicating a rigidification of this terminal end in oligomer **7**.

In the case of **7**, ^3J(N′H, $^{\alpha}$CH^1) and ^3J(N′H, $^{\alpha}$CH^2) constants[29] were extracted for all residues except residue 1 (see Table S12 in the Supporting Information). Residues 2−6 exhibited large ^3J(N′H, $^{\alpha}$CH^1) (≥9.0 Hz) and small ^3J(N′H, $^{\alpha}$CH^2) (≤4.8 Hz) constants in agreement with N′H being *antiperiplanar* to $^{\alpha}$CH^1 and *synclinal* to $^{\alpha}$CH^2 all along the backbone.

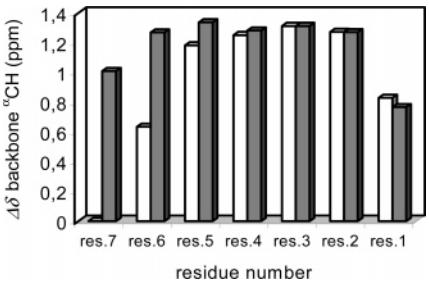

Figure 5. Chemical shift difference ($\Delta\delta$) between geminal $^{\alpha}$CH protons in oligoureas **4** (white bars) and **7** (gray bars) for residues 1−7 as determined by ^{1}H NMR in CD_3OH.

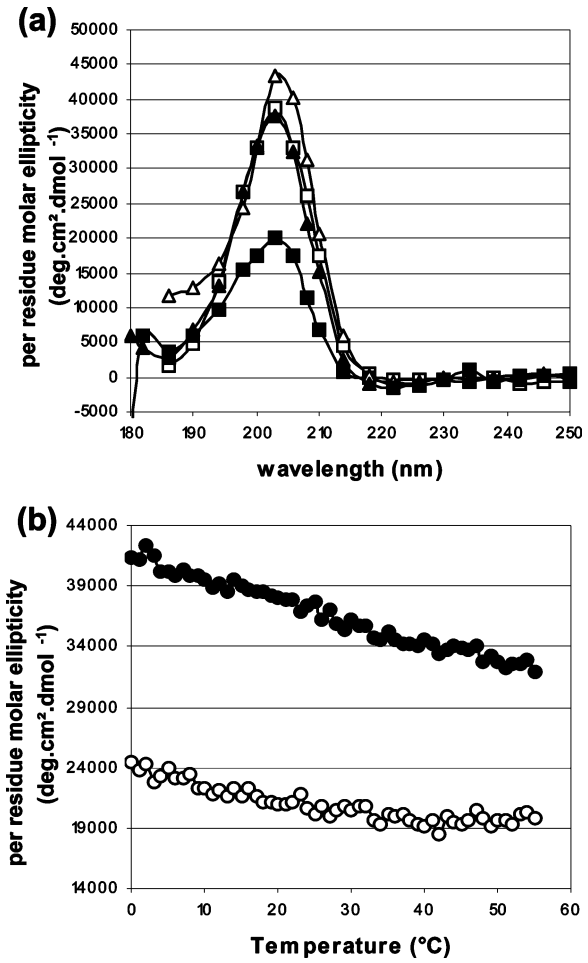

Figure 6. A comparison of the CD spectra of **4** and **7**. (a) CD spectra recorded in MeOH and TFE at room temperature at a concentration of 0.5 mM: **4** in MeOH (□); **4** in TFE (■); **7** in MeOH (△); **7** in TFE (▲). (b) CD temperature scan of **4** (○) and **7** (●) in TFE at λ = 203 nm between 0 and 55 °C.

The CD spectrum of oligomer **7** recorded in MeOH at 0.5 mM exhibited the maximum at 203 nm, and the molar ellipticity value per urea bond at this wavelength was slightly increased compared to that of **4** (4.3×10^4 versus 3.9×10^4 deg·cm^2·dmol^{-1}) (Figure 6a). Temperature-dependent CD measurements did not reveal a strong difference between **4** and **7** (Figure S11 in the Supporting Information). In both cases, the intensity of the maximum at 203 nm decreased linearly and no cooperative breakup of the structure was observed in this temperature range, thus suggesting that these oligoureas undergo noncooperative unfolding.

(31) (a) Stilbs, P. *Acta Chem. Scand.* **1971**, *25*, 2635−2642. (b) Stilbs, P.; Forsén, S. *J. Phys. Chem.* **1971**, *75*, 1901−1902. (c) Filleux-Blanchard, M. L.; Durand, A. *Org. Magn. Reson.* **1971**, *3*, 187−191. (d) Filleux-Blanchard, M. L.; Durand, A. *Bull. Soc. Chim. Fr.* **1972**, *12*, 4710−4715. (e) Martin, M. L.; Filleux-Blanchard, M. L.; Martin, G. J.; Webb, G. A. *Org. Magn. Reson.* **1980**, *13*, 396−402. (f) Haushalter, K. A.; Lau, J.; Roberts, J. D. *J. Am. Chem. Soc.* **1996**, *118*, 8891−8896.
(32) Semetey, V.; Hemmerlin, C.; Didierjean, C.; Schaffner, A.-P.; Giner, A. G.; Aubry, A.; Briand, J.-P.; Marraud, M.; Guichard, G. *Org. Lett.* **2001**, *3*, 3843−3846.
(33) (a) Jimenez Blanco, J. L.; Benito, J. M.; Mellet, C. O.; Garcia Fernandez, J. M. *Org. Lett.* **1999**, *1*, 1217−1220. (b) Ortiz Mellet, C.; Moreno Marin, A.; Jimenez Blanco, J. L.; Garcia Fernandez, J. M.; Fuentes, J. *Tetrahedron: Asymmetry* **1994**, *5*, 2325−2334.

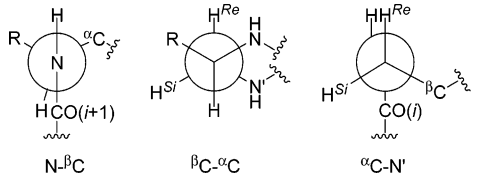

Figure 7. Idealized conformations around N−$^{\beta}$C (residues 1−7), $^{\alpha}$C−$^{\beta}$C (residues 1−7), and $^{\alpha}$C−N′ (residues 2−6) bonds in **7** deduced from NMR experiments recorded in CD_3OH at 293 K.

In contrast, a marked difference between **4** and **7** was observed when recording CD spectra were recorded in TFE (Figure 6). While the CD spectrum of **7** recorded between 179 and 250 nm still displayed a strong maximum at 203 nm (3.7×10^4 deg·cm^2·dmol^{-1}), the intensity of the maximum in the CD spectrum of **4** experienced a severe decrease in this solvent (2.0×10^4 versus 3.9×10^4 deg·cm^2·dmol^{-1} in MeOH). This difference in ellipticity at 203 nm between **4** and **7** was maintained in the temperature range between 0 and 55 °C (Figure 6b).

Like in MeOH, the shape (see Figures S12 and S13 in the Supporting Information) of the spectra of **4** and **7** in TFE was not affected by temperature changes and the ellipticity value at 203 nm decreased slowly with a temperature increase (ca 172 deg·cm^2·dmol^{-1}·K^{-1} for **7**), thus suggesting that dominant conformations at least in **7** are thermally stable. Altogether these CD results indicate (i) that acylation of the amino-terminal end (i.e., capping) of oligoureas by alkyl isocyanates may significantly stabilize one single dominant conformation of the urea backbone and (ii) that TFE may be more appropriate than MeOH to disciminate oligourea sequences on the basis of conformational stability. The apparent destabilizing effect of TFE in the case of **4** was not expected because TFE provides a lower dielectric environment (ϵ 26.1) than MeOH (ϵ 32.7), which should favor intramolecular H-bonding. In α-peptides, TFE is generally classified as a stronger promoter of helical folding than MeOH.[34]

NMR Structure Refinement for 7. Information on the geometry of the $^{\alpha}$C−$^{\beta}$C bond as well as on the identity of diastereotopic $^{\alpha}$CH^2 and $^{\alpha}$CH^1 protons[29] was gathered from DQF-COSY and ROESY experiments recorded at 293 K. Although the extraction of $^3J(^{\beta}$CH, $^{\alpha}$CH) constants was not possible because of overlaps in the $^{\beta}$CH/$^{\alpha}$CH region, the absence of a cross-peak between $^{\beta}$CH and the downfield $^{\alpha}$CH proton ($^{\alpha}$CH^1) in DQF-COSY and the presence of a strong cross-peak with $^{\alpha}$CH^2 indicated that $^{\alpha}$CH^1 and $^{\alpha}$CH^2 exhibit small and large coupling constants with $^{\beta}$CH, respectively. In addition, the intraresidue NOE between $^{\alpha}$CH^1 and NH was systematically weaker than the corresponding $^{\alpha}$CH^2/NH NOE (data not shown). As previously discussed,[14b] only one conformation around $^{\alpha}$C−$^{\beta}$C fulfills these experimental observations, and as a result $^{\alpha}$CH^1 could be assigned as $^{\alpha}$CH^{si}. The resulting idealized conformation around $^{\alpha}$C−$^{\beta}$C together with the preferential conformations around N−$^{\alpha}$C and $^{\alpha}$C−N′ bonds are shown in Figure 7.

Inspection of the 23 interesidue NOEs extracted from ROESY experiments at 293 K (Table S14 in the Supporting Information) revealed the presence for $i = 1-5$ of $^{\beta}$CH(i + 2)/NH(i) and $^{\beta}$CH(i + 2)/N′H(i) NOEs characteristic of a 2.5 helical conformation. Unexpectedly, four N′H(i + 1)/$^{\beta}$CH(i) NOEs of medium ($i = 6$ and 7) and strong ($i = 2$ and 3) intensities were observed (see Figure 8a,b). The strong intensity of the N′H(3)/$^{\beta}$CH(2) and N′H(4)/$^{\beta}$CH(3) NOEs probably reflects isomerization of the urea bond between residues 2 and 3 as well as 3 and 4. These NOEs as well as collected J values were used as distance and dihedral angle restraints, respectively, in a 100 ps simulated annealing protocol using the AMBER7 suite of programs.

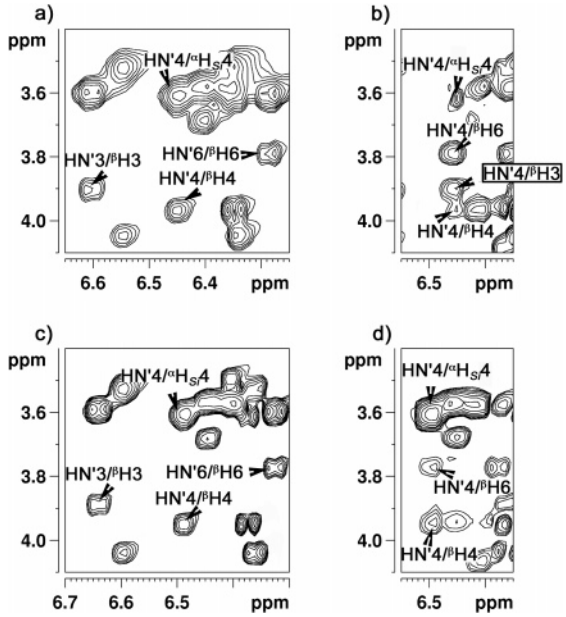

Figure 8. Selected NOEs observed for **7** in CD_3OH at 293 and 280 K. (a) Part of the TOCSY spectrum at 293 K showing N′H(i)/$^{\beta}$CH(i) for $i = 3$, 4, and 6. (b) Part of the ROESY experiment at 293 K ($\tau_m = 350$ ms). The $^{\beta}$CH(6)/N′H(4) NOE cross-peak is representative of the set of (i)−(i + 2) NOEs characteristic of the 2.5 helical structure. The strong cross-peak between N′H(4) and $^{\beta}$CH(3) is consistent with the presence of a *Z,E* urea rotamer between residues 3 and 4. (c) Part of the TOCSY spectrum at 280 K. (d) Part of the ROESY spectrum recorded at 280 K revealing the absence of the N′H(4) and $^{\beta}$CH(3) NOE cross-peak.

Calculations converged well and yielded a set of 20 structures with no NOE violation >0.3 Å and no dihedral angle violation >5°. Although the structure was grossly similar to the helical fold determined for oligomers in pyridine (Figure 9), most conformers (16 out of 20) contained a *Z,E* urea rotamer between residues 3 and 4. The mean value for the O(4)−C(4)−N(3)−H(3) torsion angle for the 20 conformers of lowest energy after simulated annealing was 57.5°. No isomerization between residues 2 and 3 was observed. Although this set of NOEs is consistent with a single helical conformation, it is more likely that the 2.5 helix is in equilibrium with the partially folded conformation in which *Z*−*E* rotamer interconversion occurs to various degrees, the *E,Z* to *Z,Z* relative population being unknown. Restrained simulated annealing in the absence of N′H(i + 1)/$^{\beta}$CH(i) NOEs yielded a closely related helical structure with all urea bonds in the *Z,Z* conformation (rms deviations for all heavy backbone atoms were 0.39 ± 0.08 Å for residues 2−6). With the aim to freeze or slow the izomerization process, ROESY experiments were recorded at 280 K. At this temperature, N′H(i + 1)/$^{\beta}$CH(i) NOEs were not observed (see Figure 8c,d) and the 15 interesidue NOEs (Table S15 in the Supporting Information) were all compatible with the 2.5 helical structure. The corresponding bundle of the 20

(34) (a) Hirota, N.; Mizuno, K.; Goto, Y. *J. Mol. Biol.* **1998**, *275*, 365−78. (b) Hirota, N.; Mizuno, K.; Goto, Y. *Protein Sci.* **1997**, *6*, 416−421.

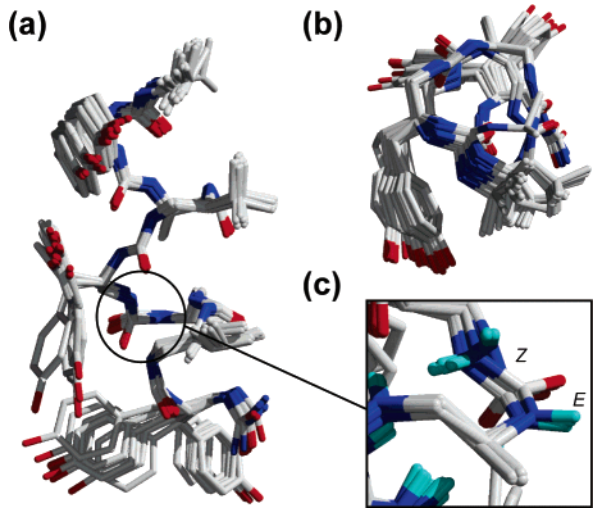

Figure 9. Conformational analysis of oligourea **7** at 293 K, a bundle of the 20 best NMR structures of lowest energy: (a) viewed along the main helix axis; (b) viewed from the top; (c) a closer view of the *Z*,*E* urea rotamer between residues 3 and 4 present in 16 of the 20 conformers of the bundle. The mean value for the O(4)−C(4)−N(3)−H(3) torsion angle for the 20 conformers of lowest energy was 57.5°. Rms deviations for all heavy backbone atoms from a mean structure were 0.40 ± 0.06 Å for residues 1−7 and 0.39 ± 0.05 Å for residues 2−6.

best NMR structures of lowest energy is shown in the Supporting Information (Figure S14). The mean values for the O(*i*)−C(*i*)−N(*i* + 1)−H(*i* + 1) torsion angle which are between ±164° and ±178° are characteristic of *Z*,*Z* urea conformers. Examination of the C═O(*i*)···N′H(*i* − 2) and C═O(*i*)···NH(*i* − 3) hydrogen-bonding patterns in **7** based on statistical analysis of the final 20 structures of lowest energy generated from NMR data at 280 K in CD_3OH indicates that the 2.5 helical structure is less regular than the one determined for **4** in pyridine (compare Tables S17 and S18 in the Supporting Information).

Molecular Dynamics Simulations. MD simulations of both oligomers **4** and **7** were conducted in explicit solvent (pyridine for oligomer **4**, methanol for oligomer **7**). The right-handed 2.5 helix observed by NMR for the two oligoureas proved to be stable when simulated without any restraints in an explicit solvent box. Atomic fluctuations, calculated over the last 900 ps on 1800 snapshots from the time-averaged conformation, were very small for main-chain atoms (lower than 20 $Å^2$ for oligomer **4** and 30 $Å^2$ for oligomer **7**), indicating a very stable fold (Figure 10a,b). As expected, side-chain atoms, notably close to residue 7, were much more mobile than backbone atoms. It was no real surprise that oligomer **7** was significantly more flexible in methanol than heptamer **4** in pyridine. For both molecules, the MD snapshots exhibit a much more regular helical pattern than NMR structures (Tables S19 and S20 in the Supporting Information). The dissymmetry observed by NMR between the frequencies of C═O(*i*)···N′H(*i* − 2) and C═O(*i*)···NH(*i* − 3) H-bonds, the former being significantly lower than the latter (Tables S16 and S18), is no longer observed in MD structures (Tables S19 and S20 in the Supporting Information). Notably, *Z*−*E* izomerization of the urea bond linking monomers 3 and 4 in oligomer **7** disappeared as soon as the NMR restraints were given less weight in the MD simulation (Figure 10c). As a consequence, the differences observed in the main-chain atoms of both oligomers **4** and **7** were significantly reduced after MD simulations (rmsd values over heavy main-chain atoms from residues 2 to 6 were 1.45 and 0.88 Å for the averaged NMR and MD structures, respectively).

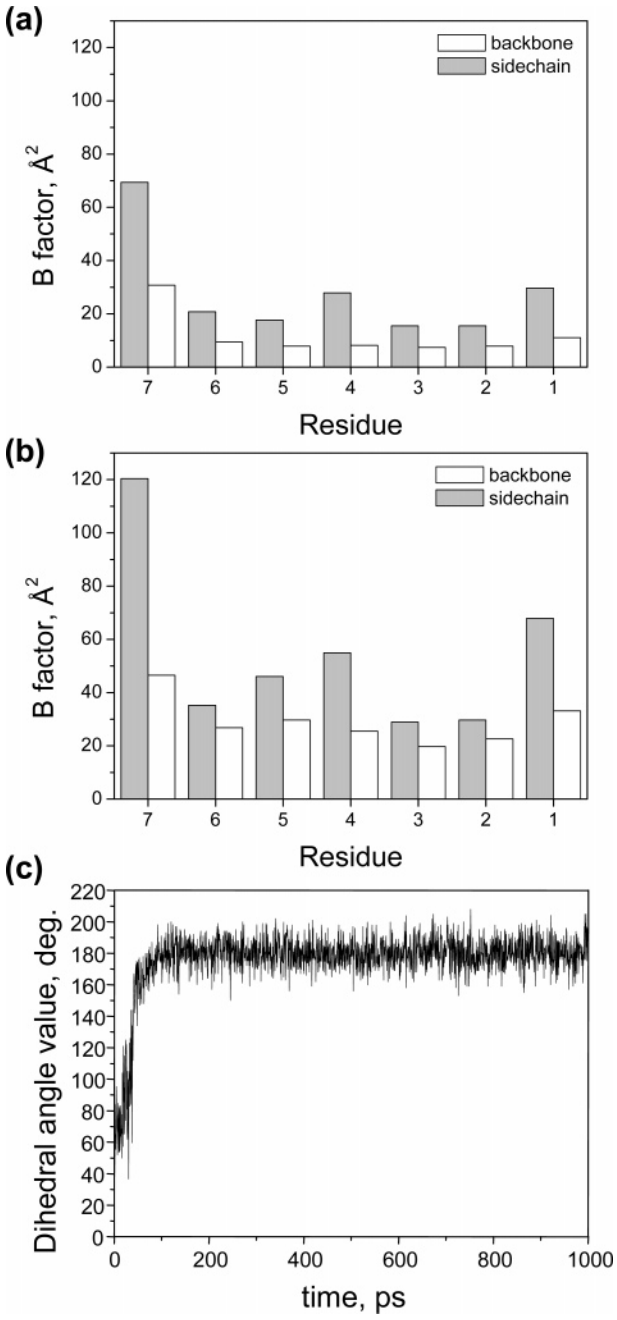

Figure 10. Analysis of MD trajectories of oligomers **4** and **7** in explicit solvent. Atomic fluctuations (transformed into thermal *B* factors) for backbone and side-chain atoms were calculated over 1800 conformations from a time-averaged structure for (a) heptamer **4** in pyridine-d_5 and (b) oligomer **7** in CD_3OH. (c) Time course of the dihedral angle value for the amide bond linking residues 3 and 4 of oligomer **7**.

Conclusions

We have performed a careful spectroscopic characterization of enantiopure *N*,*N*′-linked oligoureas ranging in length from tetramer (**1**) to nonamer (**5**) using both NMR and CD in MeOH. A number of conclusions can be drawn from these data: (i) Both the molar ellipticity per urea bond of the broad extremum near 203 nm (CD) and the chemical shift difference between geminal $^{\alpha}$CH protons (NMR) increase with oligourea chain length to reach an asymptotic value around 7−9 residues. This trend

indicates that seven residues might be sufficient for the formation of a stable 2.5 helix. (ii) While heptamer **4** adopts a stable 2.5 helical structure in pyridine, NMR experiments in MeOH rather suggest an equilibrium between the 2.5 helical conformation and interconverting folding patterns with various proportions of urea *cis*−*trans* rotamers. (iii) Removal of the positive charge at the N-terminus of **4** by capping with an alkyl isocyanate significantly increases the 2.5 helical population. The stabilization effect could be due to both the suppression of an unfavorable electrostatic interaction and the formation of an extra H-bond involving the added H-bond acceptor. (iv) Temperature-dependent CD measurements suggest that *N*,*N*′-oligoureas, like β-peptides,[35] undergo noncooperative unfolding upon heating. These observations will hopefully provide a base for the design of oligoureas with interesting biological activities as well as for future studies on helical folding propensity of oligoureas in an aqueous environment. This study also raised a number of questions such as the generality of the urea *cis*−*trans* interconversion as well as its detailed impact on helical folding propensity and helix stability. The strong solvent effect observed by CD (TFE versus MeOH) on heptamer **4** is not fully understood but suggests that TFE would give more selective information than MeOH on the folding propensity of oligoureas.

Important factors other than chain length and capping can be manipulated to influence (helical) folding of oligoureas and strengthen our understanding of this class of foldamers. For example, the conformational preference of β- and γ-peptides has been shown to depend in a striking manner on the substitution pattern and relative configuration of their amino acid constituents. While $\beta^{2,3}$-amino acids of *like* configuration exert a strong stabilizing effect on the 3_{14} helical structure of β-peptides,[4b,36] the conformational preferences of "*mixed*" β-peptides containing both β^3- and β^2-amino acid residues in their sequence[6c] differ markedly from those of the corresponding homopolymers consisting exclusively of β^3- or β^2-amino acid residues. Similarly, the residue subsitution pattern of oligourea monomers is certainly an important structural feature that is worth being addressed in future development of this work.

Acknowledgment. We thank Professor J. Sandström for helpful discussions. This work received financial support from CNRS, Région Alsace, and BIO DELIVERY SYSTEMS. A.V. is grateful for support from the Région Alsace and BIO DELIVERY SYSTEMS. The dichrograph was purchased with funds provided by the Région Alsace, BIO DELIVERY SYSTEMS, and CNRS. Use of the NMR facilities of the Service Commun de Biophysicochimie des Interactions Moléculaires, Université de Nancy, was greatly appreciated.

Supporting Information Available: Nomenclature used for designation of backbone and side-chain protons, 1D ^{1}H NMR spectra of **1**−**5** and **7**, tables with coupling constants and chemical shifts, tables with interesidue NOEs for **4** and **7**, CD spectra of **4** at different concentrations, temperature-dependent CD studies of **4** and **7**, absorption spectra in MeOH, structure calculation for **7** at 280 K, and hydrogen-bonding pattern based on analysis of structures generated from experimental NMR data and MD simulation (PDF). This material is available free of charge via the Internet at http://pubs.acs.org.

JA044392B

(35) Gademann, K.; Jaun, B.; Seebach, D.; Perozzo, R.; Scapozza, L.; Folkers, G. *Helv. Chim. Acta* **1999**, *82*, 1−11.

(36) (a) Seebach, D.; Schreiber, J. V.; Abele, S.; Daura, X.; van Gunsteren, W. F. *Helv. Chim. Acta* **2000**, *83*, 34−57. (b) Raguse, T. L.; Lai, J. R.; Gellman, S. H. *Helv. Chim. Acta* **2002**, *85*, 4154−4164.